# High-field paramagnetic Meissner effect up to 14 T in melt-textured $YBa_2Cu_3O_{7-\delta}$

Dias, F. T.; Vieira, V. N.; Wolff-Fabris, F.; Kampert, E.; Gouvea, C. P.; Campos, A. P. C.; Archanjo, B. S.; Schaf, J.; Obradors, X.; Puig, T.;

Originally published:

March 2016

**Physica C 525(2016), 105-110**

DOI: https://doi.org/10.1016/j.physc.2016.03.013

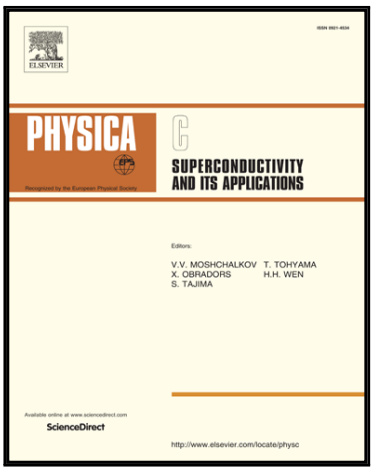


# High-field paramagnetic Meissner effect up to 14 T in melt-textured $YBa_2Cu_3O_{7-\delta}$

F.T. Dias , V.N. Vieira , F. Wolff-Fabris , E. Kampert , C.P. Gouvêa , A.P.C. Campos , B.S. Archanjo , J. Schaf , X. Obradors , T. Puig , J.J. Roa , B.K. Sahoo

PII: S0921-4534(16)30010-7
DOI: 10.1016/j.physc.2016.03.013
Reference: PHYSC 1252987

To appear in: *Physica C: Superconductivity and its applications*

Received date: 22 March 2016
Accepted date: 23 March 2016

Please cite this article as: F.T. Dias , V.N. Vieira , F. Wolff-Fabris , E. Kampert , C.P. Gouvêa , A.P.C. Campos , B.S. Archanjo , J. Schaf , X. Obradors , T. Puig , J.J. Roa , B.K. Sahoo , High-field paramagnetic Meissner effect up to 14 T in melt-textured $YBa_2Cu_3O_{7-\delta}$, *Physica C: Superconductivity and its applications* (2016), doi: 10.1016/j.physc.2016.03.013

Highlights

- A persistent paramagnetic Meissner effect up to 14 T.
- The PME with a slight tendency to saturate in high magnetic fields.
- Strong time effects causing a paramagnetic relaxation dependent on the cooling rate.

# High-field paramagnetic Meissner effect up to 14 T in melt-textured $YBa_2Cu_3O_{7-\delta}$

F.T. Dias[a,*], V.N. Vieira[a]
[a] *Instituto de Física e Matemática, Universidade Federal de Pelotas, Caixa Postal 354, 96010-900, Pelotas, Rio Grande do Sul, Brazil*

F. Wolff-Fabris[b], E. Kampert[b]
[b] *Dresden High Magnetic Field Laboratory, Helmholtz-Zentrum Dresden-Rossendorf, 01314, Dresden, Germany*

C.P. Gouvêa[c], A.P.C. Campos[c], B.S. Archanjo[c]
[c] *National Institute of Metrology, Quality and Technology (Inmetro), Material Metrology Division, 25250-020, Brazil*

J. Schaf[d]
[d] *Instituto de Física, Universidade Federal do Rio Grande do Sul, 91501-970, Porto Alegre, Rio Grande do Sul, Brazil*

X. Obradors[e], T. Puig[e]
[e] *Institut de Ciència de Materials de Barcelona, CSIC, Universitat Autònoma de Barcelona, 08193, Bellaterra, Spain*

J.J. Roa[f]
[f] *Departamento de Ciencia de Materiales e Ingeniería Metalúrgica, Universitat Politècnica de Catalunya, 08028, Barcelona, Spain*

B.K. Sahoo[g]
[g] *Goverment College (Autonomous), 759143, Angul, Odisha, India*

Corresponding author: F. T. Dias
E-mail address: fabio.dias@ufpel.edu.br
Alternative e-mail: diasft@gmail.com

ABSTRACT

We have performed magnetization experiments in a melt-textured $YBa_2Cu_3O_{7-\delta}$ (Y123) sample with $Y_2BaCuO_5$ (Y211) inclusions, under magnetic fields up to 14 T applied parallel or perpendicular to the *ab* plane. Magnetic anisotropy and paramagnetic moments were observed in both FC (field-cooling) and FCW (field-cooled warming) procedures and these features correspond to the so-called High-Field Paramagnetic Meissner Effect (HFPME). The HFPME effect increases monotonically as the magnetic field rises and a strong paramagnetic relaxation, toward increasing paramagnetic moment was additionally observed as a function of time. Microscopy analysis revealed a complex and correlated microstructure of the Y211 particles. These correlated defects are well known to cause strong flux pinning. Our results suggest a scenario of strong flux compression within weak or non-superconducting regions of the samples, developed as a consequence of the Meissner effect and assisted by strong flux pinning by the Y211 particles. This scenario is observed up to 14 T and clearly persists beyond.

**Keywords:** paramagnetic Meissner effect, vortex pinning, magnetic relaxation, magnetic flux compression

## 1. Introduction

The high-$T_c$ superconductors have been extensively studied since their discovery [1] and the $YBa_2Cu_3O_{7-\delta}$ superconductor [2] is among the most investigated materials. Several techniques have been employed in order to prepare such materials for technological applications. Melt-texturing techniques [3,4,5] are employed to prepare bulk materials with large critical current density, necessary for such applications. The strong magnetic flux pinning, presented by the melt-textured superconductors doped with non-superconducting particles [6], is a fundamental feature, when these materials are intended to be used in devices under high magnetic fields.

Regarding the magnetic properties, some superconducting materials do not exhibit the conventional Meissner effect. In these cases the material does not exhibit a diamagnetic behavior as it is cooled below the critical temperature $T_C$, but reveals a curious paramagnetic response in low fields (up to $10^{-3}$ T) known as Paramagnetic Meissner Effect (PME), or Wohlleben effect [7,8,9]. An enormous effort has been made in order to investigate the cause of this effect and it has been observed in low-$T_C$ superconductors, such as Nb [10,11,12], high-$T_C$ superconductors, such as $Bi_2Sr_2Ca_1Cu_2O_x$ [7,13,14] and $YBa_2Cu_3O_{7-\delta}$ [15,16], multiphase alloys [17], superlattices [18], organic compounds [19] and in pure Pb [20]. The effect shows itself apparently indifferent to the employed growth technique and has been observed in sintered samples [21], melt-textured samples [22,23], single-crystals [23,24], and thin films [12,25]. Therefore, a more detailed understanding of the existence and origin of the PME still remains to be found.

In this communication we present a detailed study of the anisotropic High-Field Paramagnetic Meissner Effect (HFPME), observed in magnetization measurements performed under magnetic fields up to 14 T, using a melt-textured $YBa_2Cu_3O_{7-\delta}$ (Y123) sample grown by Bridgman technique with the addition of $Y_2BaCuO_5$ (Y211) particles. Our study was made by magnetization measurements as a function of temperature, M(T), while cooling the sample under field (FC procedure) as well as warming after field cooling (FCW procedure). Magnetic relaxation studies also have revealed a strong time dependence of the FC magnetic moment. Our findings cannot be interpreted as an usual paramagnetic effect, due to polarization of atomic Copper moments in the Y211 particles, but suggest that the HFPME is dominantly a magnetic flux compression phenomenon [26] taking place in a scenario of strong flux pinning, caused by the Y211 particles dispersed in the samples.

## 2. Experimental details

The melt-textured material was grown by Bridgman technique [27,28,29,30,31,32] with 30 wt.% of Y211 precipitates, and the dimensions of our sample was approximately 0.6 mm x 0.8 mm x 2.0 mm, with the largest side found to be along the *c*-axis. The structural and microscopic characteristics of the sample were obtained by scanning electron microscopy (SEM) using a dual-beam FEI Nova NanoLab 600 and by high-resolution transmission electron microscopy (HRTEM) carried out on a probe corrected FEI Titan 80/300 transmission electron microscope operating at 300 kV. The DC magnetization measurements as a function of temperature, M(T), were performed at the Dresden High Magnetic Field Laboratory using a 14 T Quantum Design Physical Property Measurement System (PPMS) equipped with a Vibrating Sample Magnetometer. The magnetic field was applied in a configuration either parallel or perpendicular to the *ab* plane and the magnetic

moments were measured in temperatures between 100 K and 4.2 K according to the field-cooling (FC) and field-cooled warming (FCW) procedures. In the FC procedure, the magnetic field is first turned on and the magnetization is measured while slowly cooling the sample in the constant field. In the FCW procedure the sample is first cooled in constant field and then the magnetization is measured while slowly warming the sample in the same field. The time dependence of the FC magnetic moment was additionally studied by performing magnetic relaxation experiments at fixed magnetic field and temperature.

## 3. Results

### *3.1. Microscopic analysis*

Fig. 1a shows a SEM image obtained from the sample, where Y211 particles can be seen dispersed on the surface. Fig. 1b shows a TEM image of an Y211 particle, illustrating the micro-metric character of this precipitate in our sample. The size of th Y211 precipitate is influenced by the $CeO_2$ addition during the sample growth procedure. The addition of $CeO_2$ is well known to refine the Y211 particle size and enhances the superconducting properties [30]. Fig. 1c shows a HRTEM image of Y123/Y211 interface obtained from our sample. A clean interface can be observed and no new structure is formed, which is confirmed by the fast Fourier transform (FFT) of the three distinct regions showed in the figure. The superposition of the structures is not longer than 20 nm. Fig. 1d represents a SEM image that shows a fracture produced sideways (along the *c*-axis) in order to observe the layered structure. This type of structure is responsible for the anisotropic properties and for the high values of the electric current density, typically observed in melt-textured samples [4,5]. The results seen by microscopy techniques evidence the high quality of our sample, as can be seen by the clean Y123/Y211 interface and the layered structure. The presence of Y211 particles dispersed on the superconducting matrix can act as important flux pining centers which retain the magnetic flux within the sample.

### *3.2. Magnetic measurements I: FC and FCW procedures*

Magnetic measurements M(T) are shown in Fig. 2a and 2b. Were applied magnetic fields up to 14 T accordingly to the FC and FCW procedures for either H//ab (Fig. 2a) or H//c (Fig. 2b) configurations. For magnetic fields above 2 T, applied along the *ab* plane (H//*ab*), the sample shows a strong paramagnetic Meissner effect at low temperatures. The paramagnetic moment increases monotonically as the applied magnetic field is raised up to 14 T. The measurement at 0.5 T shows a diamagnetic moment below the superconducting transition. Nevertheless, the slope of M(T) shows that a paramagnetic moment too is present, whose contribution however is not strong enough to revert the overall magnetic moment to the positive side. For magnetic fields applied along the *c*-axis the overall magnetic moment in the superconducting phase is at the negative side for the whole magnetic field range. However, in spite of the negative overall magnetic moments, there is clearly a positive magnetic contribution below the critical temperature which can be associated to a paramagnetic contribution likewise in the case of H//ab. On the other hand, this strong anisotropy of the magnetic behavior for H//ab and H//c demonstrates that the *c*-axis of the crystallites in the samples is well aligned.

Irreversibility effects can be observed in Fig. 2a and 2b where the magnitude of the FCW magnetic moment exceeds the FC magnetic moment below the superconducting transition. This result is a clear indication of time effects since FC and FCW experiments were made in temporal sequence. These results are similar to those obtained for $YBa_2Cu_3O_{7-\delta}$ superconductors [22,23,24]. One of the essential features in this work is the presence of the paramagnetic Meissner effect in such magnetic fields range.

*3.3. Magnetic measurements II: magnetic relaxation*

In order to investigate the time effects observed by the irreversibility behavior between FC and FCW measurements, we have performed magnetic relaxation experiments. Fig. 3a displays the FC magnetic relaxation observed in the sample. Note that the paramagnetic relaxation is toward higher paramagnetic moments. For H//ab, the paramagnetic response raises by almost 10% after 12,000 s. This effect is even more pronounced when the same magnetic field is applied along the *c*-axis (see inset). Several magnetic relaxation studies have been reported in the literature [12,15,22]. However, the present results constitute, together with partial results in [33], in the experimental observation of the paramagnetic Meissner effect relaxation in a magnetic field as high as 14 T.

Our PME relaxation results show a strong dependence with the cooling rate employed during the field cooling experiments. Fig. 3b shows the field-cooled magnetic relaxation after cooling at 0.5 K/min and 10 K/min to 80 K under an applied field H = 0.2 T // c. In the Fig. 3b we can clearly observe that the paramagnetic relaxation rate is larger after cooling the sample at the higher rate (10 K/min), and in this case the paramagnetic moment raises by almost 50% after 20,000 s. We have also observed (not shown here) that this behavior does not depend on the measuring temperature below Tc. The paramagnetic relaxation was confirmed for different cooling rates, magnetic fields and at several fixed temperatures (not shown here), which suggests that the time effects constitute a relevant characteristic of the observed HFPME.

## 4. Discussion

The paramagnetic Meissner effect can be observed either in low or high magnetic fields with distinct features. In the low field range of a few mT it is known as Wohlleben effect. The Wohlleben effect first increases as the magnetic field is raised, but then decreases and vanishes as the magnetic field is raised above a few mT [8,13] and the diamagnetism is established. Several models have been proposed in order to understand the low field PME. In granular superconductors some interpretations are based on the occurrence of Josephson $\pi$–junctions randomly distributed between the superconducting grains [13,34,35,36]. On the other hand, the High Field Paramagnetic Meissner Effect (HFPME) is observed on from some tenths of Tesla and increases as the magnetic field is increased [15,22,23,24]. According to some authors [12,22,25,37], the HFPME exhibits time relaxation in which the FC (field-cooled) magnetization relaxes toward an increasing value of the FC magnetic moment. The HFPME has been interpreted by models based on magnetic flux compression effects [26,38,39], where a non-equilibrium compressed flux state can be generated due to inhomogeneous temperature or inhomogeneous transition temperature throughout the sample. Alternative interpretations were proposed taking into account geometry and surface of the sample [10,11,16,40], multiply-connected superconductors [41,42,43], strong pinning effect in high-$T_C$ materials [22,23], and chiral pairing [44]. Recently the PME was described in terms of a crossover between conventional Type-I and Type-II superconductors [45]. However, in spite of the numerous efforts [46,47], there isn't yet a consistent model to explain the data obtained at high magnetic fields where the paramagnetic moments increase with the magnetic field. Moreover a field limit for the occurrence of the HFPME is not predicted.

The microscopic analysis revealed the layer structure, the presence of the $Y_2BaCuO_5$ (Y211) precipitates dispersed into the Y123 superconducting matrix and a clean interface Y123/Y211 with few nanometers. Our magnetization measurements show a strong HFPME that is reinforced when the magnetic fields is increased. The HFPME is highly anisotropic for field along the *c*-axis or the *ab* plane and more pronounced for magnetic field applied along the *ab* plane. Additionally the HFPME increases with the cooling rate and exhibits relaxation with time by which the magnetic moment of the sample is higher for the FCW procedure than for the FC one (see Fig. 2). Such

relaxation was confirmed by FC magnetic relaxation experiments up to 14 T (see Fig. 3) and may also be present for higher fields.

In our view the HFPME can be understood in terms of the flux compression phenomenon proposed by Koshelev and Larkin [26]. In order to figure out this compression mechanism, it is important to understand the origin of the Meissner effect. Bose-Einstein (BE) condensation in low temperatures takes place because of the BE phase correlation between the Cooper pairs, giving rise to a negative potential energy term corresponding to about 1 meV per Cooper pair. On condensing, the system minimizes its energy, forcing the bosonic particles to assume all the same phase and thereby establishing a phase coherent state described by the complex superconducting order parameter $\Psi = \psi(r)\, e^{i\phi}$. The vector potential associated with an applied magnetic field causes local phase displacements of the superconducting order parameter, which means phase disorder and screening currents, thereby elevating the energy of the superconducting condensate above the minimum. The excited superconducting condensate can lower its energy by expelling the magnetic field out from the superconductor, which is the Meissner effect. By the Meissner effect, type-II superconductors minimize energy, confining the magnetic field into microscopic flux tubes or expelling it out from the superconductor. However, in non-homogeneous superconductors out from the superconductor is not necessarily out from the sample. It also can mean inward, toward non-superconducting or weaker superconducting regions.

In our melt-textured $YBa_2Cu_3O_{7-\delta}$ sample an inhomogeneous scenario is easily developed during sample cooling because of inhomogeneous sample temperature and inhomogeneous superconducting transition temperature due to inhomogeneous oxygen doping or even due to the non-superconducting Y211 particles. Anyway the sample boundary cools first and becomes superconducting, thereby trapping the magnetic field already within the sample. Because of the Meissner effect, the magnetic flux will be driven out from the superconducting boundary layer toward both sides. A part will be expelled out from the sample and another part is thrust inward toward the internal non-superconducting regions. As the cooling goes on, the sample cools toward the interior and the magnetic flux gradually will be swept inward and compressed within the weaker superconducting regions. The compressed field depresses even more the local superconductivity forming a non-superconducting or weaker superconducting region in the bulk and giving rise to a paramagnetic moment. Flux sweeping and compression lets behind a low flux density region, opening space for admission of new fluxons from outside. In order to the flux compression to increase more and more, there is need of strong flux pinning backing and propping up the flux and the screening currents from behind, which is provided by the Y211 particles as well as by the Y123/Y211 interfaces. Besides the paramagnetic moment due to flux compression, polarization of the Copper moments within the Y211 particles by the compressed field also contributes to the overall paramagnetic moment. However, this contribution is only a byproduct of the magnetic field compression. Note that in the FC procedure the field already is fully within the sample and the paramagnetic contribution of the local Copper moments certainly is not a dominant effect.

The strong time dependence of the HFPME, observed in the sample for the FC and FCW procedures and also confirmed by FC magnetic relaxation experiments, is explained by the fact that the system finds it in a non-equilibrium state. The vortices near the boundary of the sample are under the pressure from outside by the applied magnetic field and stabilized from inside by flux pinning. However, as the flux has been swept inward, the external pressure may exceed the internal resistance. Assisted by thermal activation and quantum fluctuations, the fluxons may creep inward and extra magnetic flux may penetrate from outside. The FC magnetic relaxation experiments shown in the figure 3 let no doubt that additional magnetic flux penetrates the sample and that higher cooling rates produce a higher non-equilibrium state. The time dependence of the HFPME in $YBa_2Cu_3O_{7-\delta}$ samples was shown in previous works [15,22,33]. The present results show that the magnetic flux compression is very strong and that moreover the flux density within the sample increases with time and this relaxation rate increases with increasing of the (constant) applied

magnetic field.

The HFPME shows a very slow saturation tendency at high magnetic fields, as seen in Fig. 4. Fig. 4a shows results for the sample investigated in this work, at 10 K and for H//ab, while the Fig. 4b shows results in the same conditions, however for another melt-textured $YBa_2Cu_3O_{7-\delta}$ sample that showed a similar HFPME behavior (top-seeding sample in [33]). Nevertheless, if a saturation limit exists for the HFPME, it may occurs well above 14 T. In previous works [15,22,23,24] this saturation tendency could not be suggested, however, recently obtained results in an $YBa_2Cu_3O_{7-\delta}$ thin film reinforce this behavior [48]. The results obtained in this work indicate that under extremely high magnetic fields, in which the superconductivity becomes strongly depressed, flux compression eventually may collapse and the superconducting sample possibly could restore a diamagnetic response.

The superconducting condensate and the Meissner effect, confining electromagnetic fields and providing inertial mass to the photon within superconductors [49], has been an important guide to understand the Higgs Mechanism, confining weak and strong nuclear fields and providing inertial mass to the elementary particles. We believe that the observation of the HFPME in such high magnetic fields can open ways for new theoretical works taking into account the Meissner effect, flux pinning and flux dynamics in order to explain the behavior of the HFPME in high magnetic fields. It can even provide new insights in Quantum Field Theory [50].

## 5. Conclusion

We have performed magnetic measurements in a melt-textured $YBa_2Cu_3O_{7-\delta}$ (Y123) sample grown by Bridgman technique, in order to study the high-field paramagnetic Meissner effect (HFPME) in applied magnetic fields up to 14 T, parallel and perpendicular to the *ab*-plane. The magnetic measurements were performed following FC and FCW procedures and the time dependence of the HFPME was investigated by FC magnetic relaxation experiments.

The microscopic analysis revealed the presence of $Y_2BaCuO_5$ (Y211) precipitates dispersed into the Y123 superconducting matrix, and a clean interface Y123/Y211. These results also revealed a layered structure, typically observed in melt-textured samples of good quality. Our FC and FCW magnetic measurements showed strong paramagnetic moments, that increase with applied magnetic fields up to 14 T, which is one of the first observations of PME in this magnetic field range, together with previous results reported in [33]. The HFPME in our sample is highly anisotropic and more pronounced when the magnetic field is applied along the *ab* plane. We also observed strong time effects in FC and FCW magnetization measurements as well as in specific FC magnetic relaxation experiments. These results displayed a dependence on the cooling rate during the experiments, in such a way that the paramagnetic moment increases with increasing cooling rate. Interesting results on $Ti_{0.8}V_{0.2}$ system were reported [51], showing irreversibilities observed during FC and FCW magnetic measurements and a strong dependence on the cooling rate employed. These results show that the HFPME has similar characteristics in different superconducting systems.

Our results can be explained in terms of the flux compression mechanism, such as proposed by Koshelev and Larkin [26], and assisted by the strong pinning effect due to the Y211-phase and the Y123/Y211-interface. This microstructure produces an efficient pinning mechanism that can favor the flux compression in the sample, when an inhomogeneous cooling scenario is established. The HFPME also showed a slight tendency to saturate in high magnetic fields, indicating a possible limit in very high fields. We believe that the results presented in this work can be useful for constructing new models to explain the HFPME in high magnetic fields and the interactions of pinning mechanisms and vortex dynamics.

## Acknowledgements

This work was financed by the Brazilian MCTI/CNPq Universal 14/2012 (contract number 477506/2012-7). The experimental work at the HLD was supported by Euromagnet II (contract number 228043).

## 6. References

[1] J.G. Bednorz, K.A. Müller, Possible high $T_C$ superconductivity in the Ba−La−Cu−O system, Zeitschrift für Physik B 64 (1986) 189-193.

[2] M.K. Wu, J.R. Ashburn, C.J. Torng, P.H. Hor, R.L. Meng, L. Gao, Z.J. Huang, Y.Q. Wang, C.W. Chu, Superconductivity at 93 K in a new mixed-phase Y-Ba-Cu-O compound system at ambient pressure, Phys. Rev. Lett. 58 (1987) 908-910.

[3] S. Jin, T.H. Tiefel, R.C. Sherwood, R.B. van Dover, M.E. Davis, G.W. Kammlott, R.A. Fastnacht, Melt-textured growth of polycrystalline $YBa_2Cu_3O_{7-\delta}$ with high transport $J_C$ at 77 K, Phys. Rev. B 37 (1988) 7850-7853.

[4] G. Desgardin, I. Monot, B. Raveau, Texturing of high-$T_c$ superconductors, Supercond. Sci. Technol. 12 (1999) R115-R133.

[5] D.A. Cardwell, Processing and properties of large grain (RE)BCO, Mater. Sci. Eng. B 53 (1998) 1-10.

[6] B. Martínez, X. Obradors, A. Gou, V. Gomis, S. Piñol, J. Fontcuberta, H. Van Tol, Critical currents and pinning mechanisms in directionally solidified $YBa_2Cu_3O_7$-$Y_2BaCuO_5$ composites, Phys. Rev. B 53 (1996) 2797-2810.

[7] P. Svedlindh, K. Niskanen, P. Norling, P. Nordblad, L. Lundgren, B. Lönnberg, T. Lundström, Anti-Meissner effect in the BiSrCaCuO-system, Physica C 162–164 (1989) 1365-1366.

[8] S. Riedling, G. Bräuchle, R. Lucht, K. Röhberg, H.v. Löhneysen, H. Claus, A. Erb, G. Müller-Vogt, Observation of the Wohlleben effect in $YBa_2Cu_3O_{7-\delta}$ single crystals, Phys. Rev. B 49 (1994) 13283-13286.

[9] D. Khomskii, Wohlleben Effect (Paramagnetic Meissner Effect) in High-Temperature superconductors, J. Low Temp. Phys. 95 (1994) 205-223.

[10] D.J. Thompson, L.E. Wenger, J.T. Chen, Paramagnetic meissner effect in conventional Nb superconductors, J. Low Temp. Phys. 105 (1996) 509-514.

[11] M.S.M. Minhaj, D.J. Thompson, L.E. Wenger, J.T. Chen, Paramagnetic Meissner effect in a niobium disk, Physica C 235-240 (1994) 2519-2520.

[12] A. Terentiev, D.B. Watkins, L.E. De Long, D.J. Morgan, J.B. Ketterson, Paramagnetic relaxation and Wohlleben effect in field-cooled Nb thin films, Phys. Rev. B 60 (1999) R761-R764.

[13] W. Braunisch, N. Knauf, V. Kataev, S. Neuhausen, A. Grütz, A. Kock, B. Roden, D. Khomskii, D. Wohlleben, Paramagnetic Meissner effect in Bi high-temperature superconductors, Phys. Rev.

Lett. 68 (1992) 1908-1911.

[14] E.L. Papadopoulou, P. Nordblad, P. Svedlindh, R. Schöneberger, R. Gross, Magnetic Aging in $Bi_2Sr_2CaCu_2O_8$ Displaying the Paramagnetic Meissner Effect, Phys. Rev. Lett. 82 (1999) 173-176.

[15] F.T. Dias, P. Pureur, P. Rodrigues Jr., X. Obradors, Paramagnetic Meissner effect at high fields in melt-textured $YBa_2Cu_3O_{7-\delta}$, Physica C 354 (2001) 219-222.

[16] R. Lucht, H.v. Löhneysen, H. Claus, M. Kläser, G. Müller-Vogt, Surface-sensitive paramagnetic Meissner effect in $YBa_2Cu_3O_x$ single crystals, Phys. Rev. B 52 (1995) 9724-9726.

[17] S. Chu, A.J. Schwartz, T.B. Massalski, D.E. Laughlin, Extrinsic paramagnetic Meissner effect in multiphase indium-tin alloys, Appl. Phys. Lett. 89 (2006) 111903 (3pp).

[18] M.A.L. de la Torre, V. Peña, Z. Sefrioui, D. Arias, C. Leon, J. Santamaria. J.L. Martinez, Paramagnetic Meissner effect in $YBa_2Cu_3O_7 / La_{0.7}Ca_{0.3}MnO_3$ superlattices, Phys. Rev. B 73 (2006) 052503 (4pp).

[19] A.G. Lebed, Paramagnetic intrinsic Meissner effect in layered superconductors, Phys. Rev. B 78 (2008) 012506 (4pp).

[20] D. Brandt, C. Binns, S.J. Gurman, G. Torricelli, D.S.W. Gray, Paramagnetic Meissner Transitions in Pb Films and the Vortex Compression Model, J. Low Temp. Phys. 163 (2011) 170-175.

[21] J. Magnusson, J.-O. Andersson, M. Björnander, P. Nordblad, P. Svedlindh, Time dependence of the paramagnetic Meissner effect: Comparison between model calculations and experiments, Phys. Rev. B 51 (1995) 12776-12781.

[22] F.T. Dias, P. Pureur, P. Rodrigues Jr., X. Obradors, Paramagnetic effect at low and high magnetic fields in melt-textured $YBa_2Cu_3O_{7-\delta}$, Phys. Rev. B 70 (2004) 224519 (9pp).

[23] F.T. Dias, V.N. Vieira, M.L. de Almeida, A.L. Falck, P. Pureur, J.L. Pimentel Jr., X. Obradors, Paramagnetic Meissner effect at high fields in YCaBaCuO single crystal and melt-textured YBaCuO, Physica C 470 (2010) S111-S112.

[24] A.I. Rykov, S. Tajima, F.V. Kusmartsev, High-field paramagnetic effect in large crystals of $YBa_2Cu_3O_{7-\delta}$, Phys. Rev. B 55 (1997) 8557-8563.

[25] D.A. Luzhbin, A.V. Pan, V.A. Komashko, V.S. Flis, V.M. Pan, S.X. Dou, P. Esquinazi, Origin of paramagnetic magnetization in field-cooled $YBa_2Cu_3O_{7-\delta}$ films, Phys. Rev. B 69 (2004) 024506 (7pp).

[26] A.E. Koshelev, A.I. Larkin, Paramagnetic moment in field-cooled superconducting plates: Paramagnetic Meissner effect, Phys. Rev. B 52 (1995) 13559-13562.

[27] S. Piñol, V. Gomis, B. Martinez, A. Labarta, J. Fontcuberta, X. Obradors, Bridgman growth and enhanced critical currents in textured $YBa_2Cu_3O_7$ - $Y_2BaCuO_5$ composites, J. Alloys Compd. 195 (1993) 11-14.

[28] K. Salama, D.F. Lee, Progress in melt texturing of $YBa_2Cu_3O_x$ superconductor, Supercond. Sci. Technol. 7 (1994) 177-193.

[29] X. Obradors, R. Yu, F. Sandiumenge, B. Martinez, N. Vilalta, V. Gomis, T. Puig, S. Piñol, Directional solidification of $ReBa_2Cu_3O_7$ (Re = Y, Nd): microstructure and superconducting properties, Supercond. Sci. Technol. 10 (1997) 884-890.

[30] S. Piñol, F. Sandiumenge, B. Martínez, V. Gomis, J. Fontcuberta, X. Obradors, E. Snoeck, C. Roucau, Enhanced critical currents by $CeO_2$ additions in directionally solidified $YBa_2Cu_3O_7$, Appl. Phys. Lett. 65 (1994) 1448-1450.

[31] D. Müller, M. Ullrich, K. Heinemann, H.V. Freyhardt, Microstructure of melt-textured $YBa_2Cu_3O_{7-\delta}$, Physica C 220 (1994) 67-73.

[32] F. Sandiumenge, S. Piñol, X. Obradors, E. Snoeck, C. Roucau, Microstructure of directionally solidified high-critical-current $YBa_2Cu_3O_7$-$Y_2BaCuO_5$ composites, Phys. Rev. B 50 (1994) 7032-7045.

[33] C.P. Gouvêa, F.T. Dias, V.N. Vieira, D.L. Silva, J. Schaf, F. Wolff-Fabris, J.J.R. Rovira, Paramagnetic Meissner Effect and Strong Time Dependence at High Fields in Melt-Textured High-$T_C$ Superconductors, J. Kor. Phys. Soc. 62 (2013) 1414-1417.

[34] B. Freitag, B. Büchner, N. Knauf, B. Roden, H. Micklitz, A. Freimuth, V. Kataev, Characteristic microstructure in small Bi-2212 grains showing the Wohlleben effect as revealed by High-Resolution Electron Microscopy, Europhys. Lett. 45 (1999) 393-398.

[35] F.V. Kusmartsev, Destruction of the Meissner Effect in Granular High-Temperature Superconductors, Phys. Rev. Lett. 69 (1992) 2268-2271.

[36] M. Sigrist, T.M. Rice, Unusual paramagnetic phenomena in granular high-temperature superconductors - A consequence of *d*-wave pairing?, Rev. Mod. Phys. 67 (1995) 503-513.

[37] Y.V. Obukhov, The "Paramagnetic" Meissner Effect in Superconductors, J. Supercond. 11 (1998) 733-736.

[38] V.V. Moshchalkov, X.G. Qiu, V. Bruyndoncx, Paramagnetic Meissner effect from the self-consistent solution of the Ginzburg-Landau equations, Phys. Rev. B 55 (1997) 11793-11801.

[39] A.K. Geim, S.V. Dubonos, J.G.S. Lok, M. Henini, J.C. Maan, Paramagnetic Meissner effect in small superconductors, Nature 396 (1998) 144-146.

[40] P. Kostic´, B. Veal, A.P. Paulikas, U. Welp, V.R. Todt, C. Gu, U. Geiser, J.M. Williams, K.D. Carlson, R.A. Klemm, Paramagnetic Meissner effect in Nb, Phys. Rev. B 53 (1996) 791-801.

[41] F.M. Araujo-Moreira, P. Barbara, A.B. Cawthorne, C. Lobb, Reentrant ac Magnetic Susceptibility in Josephson-Junction Arrays, Phys. Rev. Lett. 78 (1997) 4625-4628.

[42] A.P. Nielsen, A.B. Cawthorne, P. Barbara, F.C. Wellstood, C. Lobb, R.S. Newrock, M.G. Forrester, Paramagnetic Meissner effect in multiply-connected superconductors, Phys. Rev. B 62 (2000) 14380-14383.

[43] P. Barbara, F.M. Araujo-Moreira, A.B. Cawthorne, C.J. Lobb, Reentrant ac magnetic susceptibility in Josephson-junction arrays: An alternative explanation for the paramagnetic Meissner effect, Phys. Rev. B 60 (1999) 7489-7495.

[44] L. Balicas, G. Li, R.R. Urbano, P. Goswami, C. Tarantini, B. Lv., P. Kuhns, A.P. Reyes, C.W. Chu, Anomalous hysteresis as evidence for a magnetic-field-induced chiral superconducting state in LiFeAs, Phys. Rev. B 87 (2013) 024512 (10pp).

[45] R.M. da Silva, M.V. Milosevic', A.A. Shanenko, F.M. Peeters, J.A. Aguiar, Giant paramagnetic Meissner effect in multiband superconductors, Sci. Rep. 5 (2015) 12695 (9pp).

[46] M.S. Li, Paramagnetic Meissner effect and related dynamical phenomena, Phys. Rep. 376 (2003) 133-223.

[47] J.J. Roa, F.T. Dias, M. Segarra, Magnetical Response and Mechanical Properties of High Temperature Superconductors, $YBa_2Cu_3O_{7-X}$ Materials, in: Y. Grigorashvili (Ed.), Superconductors – Properties, Technology, and Applications, InTech Ed., Croatia, 2012, pp. 181-218.

[48] F.T. Dias, V.N. Vieira, D.L. Silva, J.A. Aguiar, D.R.B. Valadão, X. Obradors, T. Puig, F. Wolff-Fabris, E. Kampert, Paramagnetic moments in $YBa_2Cu_3O_{7-\delta}$ nanocomposite films, Physica C 503 (2014) 175-177.

[49] P.W. Anderson, Plasmons, Gauge Invariance, and Mass, Phys. Rev. 130 (1963) 439-442.

[50] L. Dixon, From Superconductors to Supercolliders, Beam Line – Stanford Linear Accelerator Center 26 (1996) 23-30.

[51] Md. Matin, L.S. Sharath Chandra, M.K. Chattopadhyay, M.N. Singh, A.K. Sinha, S.B. Roy, High field paramagnetic effect in the superconducting state of $Ti_{0.8}V_{0.2}$ alloy, Supercond. Sci. Technol. 26 (2013) 115005 (7pp).

**Figure captions**

**Fig. 1.** (a) SEM and (b) TEM results obtained from the surface of the sample where Y211 particles can be observed at both images. (c) HRTEM bright field image showing a clean Y123/Y211 interface and the absence of any new structure. (d) SEM image showing the layered structure, typical of melt-textured samples of good quality.

**Fig. 2.** Magnetic moment as function of temperature. A strong and anisotropic paramagnetic Meissner effect is observed in high magnetic fields for (a) H//ab and (b) H//c.

**Fig. 3.** Fig. (a) shows the paramagnetic relaxation of our melt-textured $YBa_2Cu_3O_{7-\delta}$ sample. The results are expressed in terms of the normalized FC magnetic moment, where $M_0$ is the magnetic moment when t = 0 s. The inset shows that the relaxation is more pronounced when the magnetic field is applied along the *c*-axis. Fig. (b) shows that the paramagnetic relaxation rate is highly dependent on the cooling rate employed during the experiment.

**Fig. 4.** The FC paramagnetic moment, due to the HFPME, versus applied magnetic field (H//ab) at 10 K for (a) the sample investigated in this work and (b) another melt-textured sample (see text) for comparison.

FIGURES

Fig. 1

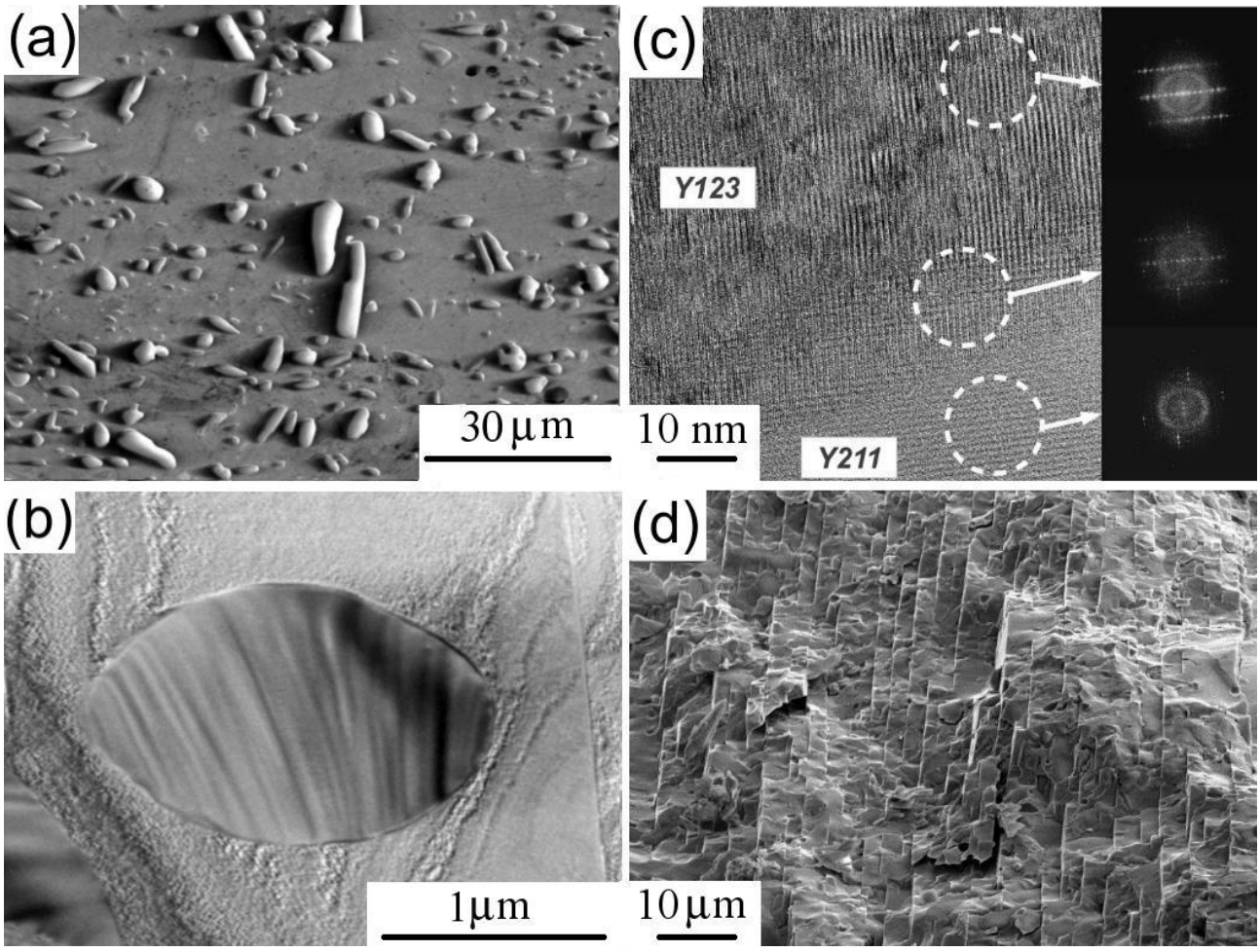

Fig. 2

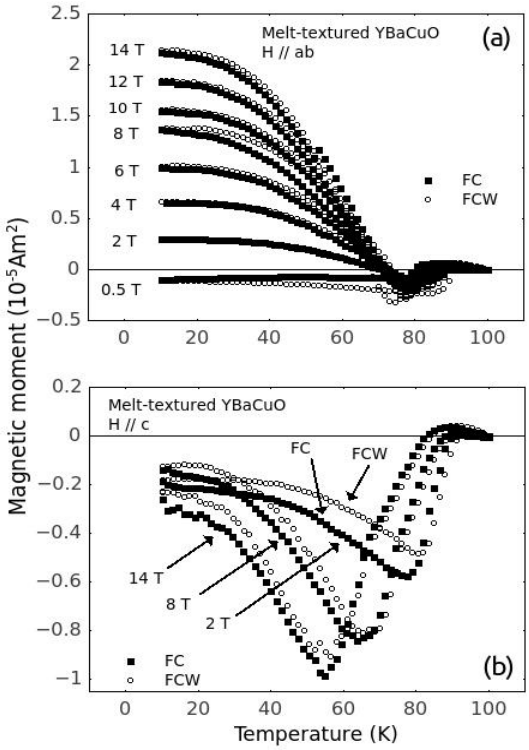
Melt-textured YBaCuO
H // ab
(a)
14 T
12 T
10 T
8 T
6 T
4 T
2 T
0.5 T
FC
FCW
Magnetic moment ($10^{-5}$Am$^2$)
Melt-textured YBaCuO
H // c
FC
FCW
14 T
8 T
2 T
(b)
Temperature (K)

Fig. 3

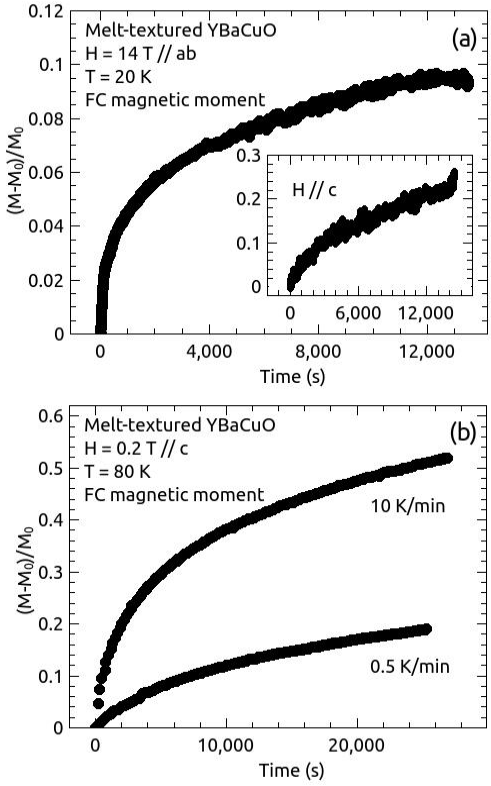
Melt-textured YBaCuO
H = 14 T // ab
T = 20 K
FC magnetic moment
(a)
H // c
(M-M$_0$)/M$_0$
Time (s)
Melt-textured YBaCuO
H = 0.2 T // c
T = 80 K
FC magnetic moment
(b)
10 K/min
0.5 K/min
(M-M$_0$)/M$_0$
Time (s)

Fig. 4

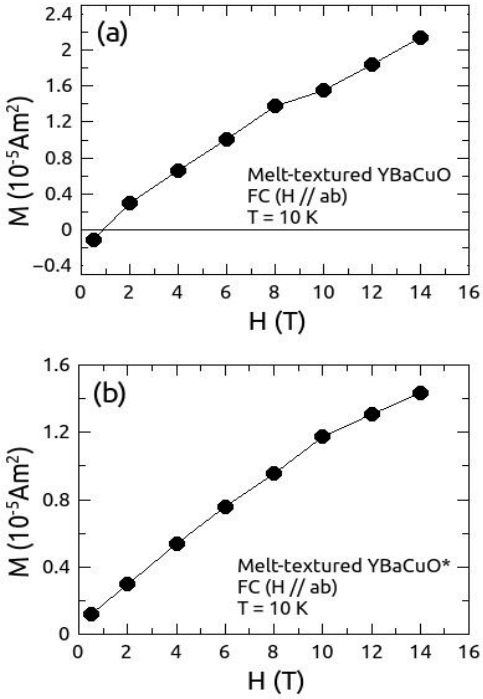
(a)
M (10$^{-5}$Am$^2$)
H (T)
Melt-textured YBaCuO
FC (H // ab)
T = 10 K
(b)
M (10$^{-5}$Am$^2$)
H (T)
Melt-textured YBaCuO*
FC (H // ab)
T = 10 K